Cylindrical and Conical Flow Regimes of Three-Dimensional Shock/Boundary-Layer Interactions

Gary S. Settles* and Hsueh-Ying Teng†
Princeton University, Princeton, New Jersey

A parametric study of three-dimensional shock/turbulent boundary-layer interactions generated by semi-infinite sweptback compression corners has revealed the existence of two characteristic flow regimes: cylindrical and conical. Experimental criteria are presented to define these regimes and their mutual boundary for one value of M_∞ (2.95). It is hypothesized that the change from one regime to another is intimately connected with the inviscid shock detachment phenomenon, and experimental evidence is given in support of this hypothesis.

Nomenclature

L_i = length along corner from model apex required for the inception of cylindrical or conical flow, cm
L_m = length of upstream influence from the corner, cm
L_{m_i} = length of upstream influence from the corner at the inception point of cylindrical or conical flow, cm
M = Mach number
P = static pressure, N/m^2
Re = freestream Reynolds number, u_∞/ν_∞, m^{-1}
Re_δ = boundary-layer thickness Reynolds number
u = mean streamwise velocity, m/s
x = distance along test surface in freestream direction, measured from plate leading edge or corner location, cm
y = distance normal to test surface in z = const planes, cm
z = transverse distance normal to x axis
Δz = transverse distance from virtual apex of conical flowfield to model apex, cm
α_{dt} = corner angle for two-dimensional shock detachment, deg
α_N = compression corner angle measured in the normal direction, deg
α_s = compression corner angle measured in the streamwise direction, deg
δ = boundary-layer thickness, cm
δ_l = local incoming boundary-layer thickness just upstream of three-dimensional interaction, cm
λ = compression corner sweepback angle measured in x-z plane, deg
λ_{co} = sweepback angle in the conical flow region, deg
λ_{cy} = sweepback angle in the cylindrical flow region, deg
λ_{cr} = sweepback angle on the conical-cylindrical boundary, deg
ν = kinematic viscosity, m^2/s
μ = Mach angle, deg

Subscripts

0 = undisturbed conditions at corner location in the absence of an interaction
∞ = freestream conditions

Figure Notation

A = apex
C = swept corner line
M = maximum upstream influence line
R = reattachment line
S = separation line

Introduction

THE interaction of a shock wave with a turbulent boundary layer is a fluid dynamics problem with both practical significance and daunting complexity. Many recent reviews[1-4] illustrate that progress has been made in understanding these interactions through experimental, analytical, and computational studies. However, there are still critical issues to be resolved, even in the simplified case of two-dimensional (2D) shock/boundary-layer interactions. For the general case of three-dimensional (3D) interactions much less is known, and an overall framework for classifying and scaling them is still lacking.

The current phase of an experimental investigation aimed at providing such a framework is reported in this paper. Specifically, it concerns the class of 3D shock/boundary-layer interactions generated by sweptback compression corners, where the sweepback angle is varied systematically from 0 deg (2D flow) to large values producing highly 3D flows. Previous papers by the authors and their colleagues have reported an exploratory study of swept corner interactions,[5] a general 3D scaling law accounting for Reynolds number effects,[6] and a collection of experimental methods for visualizing such flows.[7] The present work concerns the classification of swept corner interactions in terms of cylindrical and conical regimes.

Past studies have indicated that 3D interactions do exhibit such cylindrical and conical regimes under certain conditions. Stalker's[8] experiments with swept forward-facing steps, for example, produced cylindrically symmetric interactions. On the other hand, several investigators (e.g., Refs. 9 and 10) found conical symmetry in interactions with swept planar shock waves generated by semi-infinite fins. Zheltovodov[10] also observed a conversion from conical to cylindrical interaction symmetry as his semi-infinite fin was reduced to finite height. A similar conversion was observed to depend upon both sweepback (λ) and turning (α) angles in the exploratory swept corner study of Settles et al.[5] However, to date neither an explanation nor an explicit criterion has been suggested for this phenomenon.

Presented as Paper 82-0987 at the AIAA/ASME Third Joint Thermophysics, Fluids, Plasma and Heat Transfer Conference, St. Louis, Mo., June 7-11, 1982; submitted June 11, 1982.

*Research Engineer and Lecturer, Mechanical and Aerospace Engineering Dept. Presently Associate Professor of Mechanical Engineering, Pennsylvania State University, University Park, Pa. Member AIAA.

†Research Staff Member, Mechanical and Aerospace Engineering Dept. Presently Lecturer, Beijing Institute of Aeronautics and Astronautics, Beijing, China.

It is the present goal to provide both a plausible explanation and suitable criteria for cylindrical and conical 3D interaction regimes at swept corners and their mutual boundary. Accordingly, four specific questions will be addressed:

1) How does one determine whether an observed interaction is asymptotically cylindrical or conical?

2) What swept corner geometrical criteria determine the form and location of the cylindrical/conical regime boundary?

3) How is this boundary affected by changes in the incoming flow parameters (M_∞, Re_δ, etc.)?

4) What is the physical mechanism responsible for this boundary?

The problem is approached through a set of parametric experiments using swept compression corners. These swept corners generate a wide range of 3D shock interactions with an incoming supersonic turbulent boundary layer. The above questions are addressed through the results of these experiments.

Experimental Procedures

Wind Tunnel and Models

The experiments were performed in the Princeton University 20×20 cm High Reynolds Number Supersonic Tunnel. While some swept corner models were tested on the tunnel floor, the bulk of the data set was obtained using the flat plate test geometry shown in Fig. 1.

Swept compression corner models were mounted on this flat plate such that, regardless of sweep, their leading edges coincided at a point defined by the intersection of the streamwise and transverse datum lines at $z=5.08$ cm and $x=29.7$ cm, respectively. The only exceptions to this scheme were the corner models with $\lambda=50$, 55, and 60 deg, which had a common reference point at $z=8.89$ cm and $x=33.5$ cm, and the models tested on the tunnel floor at $z=7.62$ cm and $x=30$ cm downstream of the nozzle exit.

A parametric set of 34 compression corner models was tested, covering the ranges of sweepback angle 0 deg $\leq\lambda\leq$ 60 deg and streamwise corner angle 5 deg $\leq\alpha_s\leq$ 24 deg. All models were inset 2.54 cm from the tunnel sidewalls. The vertical thickness of the models was 5.08 cm except for $\alpha_s=5$ deg, $\lambda=45$-60 deg and $\alpha_s=10$ deg, $\lambda=45$ deg, where the thickness was 2.54 cm. The present set of corner models is an expanded version of the set previously tested and reported in Refs. 5-7.

Test Conditions

The tests were conducted at $M_\infty=2.95$ with a stagnation temperature of 261 K ±4%, a stagnation pressure of 0.689×10^6 N/m^2 ±1%, and a nominal freestream Reynolds number of 6.3×10^7/m. Fully developed, approximately adiabatic turbulent boundary layers were developed on both the flat plate and the tunnel floor. These layers met the usual wall-wake law criterion defining mean-flow equilibrium (see Ref. 6 for more detail).

The incoming boundary-layer thickness, δ_0, was 0.45 cm and 2.26 cm at the plate and floor datum line intersections, respectively. However, the growth of δ with streamwise distance caused the local incoming boundary-layer thickness δ_ℓ to vary with z for swept interactions. This nonuniform δ_ℓ effect will be taken into account later in the discussion.

Techniques and Instrumentation

The present experiments consider only the mean "footprint" of the 3D shock/boundary-layer interaction as revealed by surface flow visualization and static pressure measurements. While these data are important, they do not sufficiently address either the overall flowfield structure or the interaction unsteadiness (which are subjects of ongoing study).

Surface flow patterns were obtained by a specialized kerosene-lampblack streak technique[7] and surface pressures were read from several rows of taps connected to a computer-controlled Scanivalve bank. Extensive comparisons of these results have shown that they give essentially equivalent indications of upstream influence in a shock/boundary-layer interaction.[6] Further, flowfield visualization by localized vapor screen and conical shadowgraph methods has shown that, where a line of surface streak convergence occurs at a position near the beginning of a swept corner interaction, it is an accurate mean indicator of 3D separation of the boundary layer.[7]

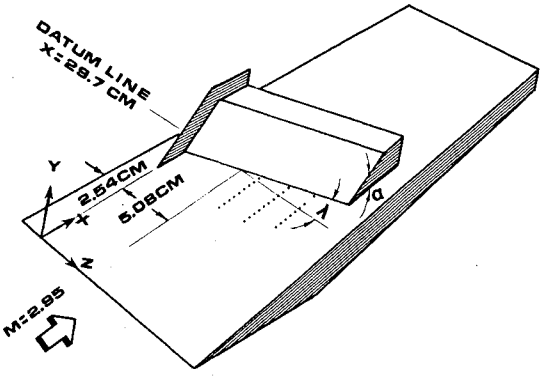

Fig. 1 Flat plate and swept corner test geometry.

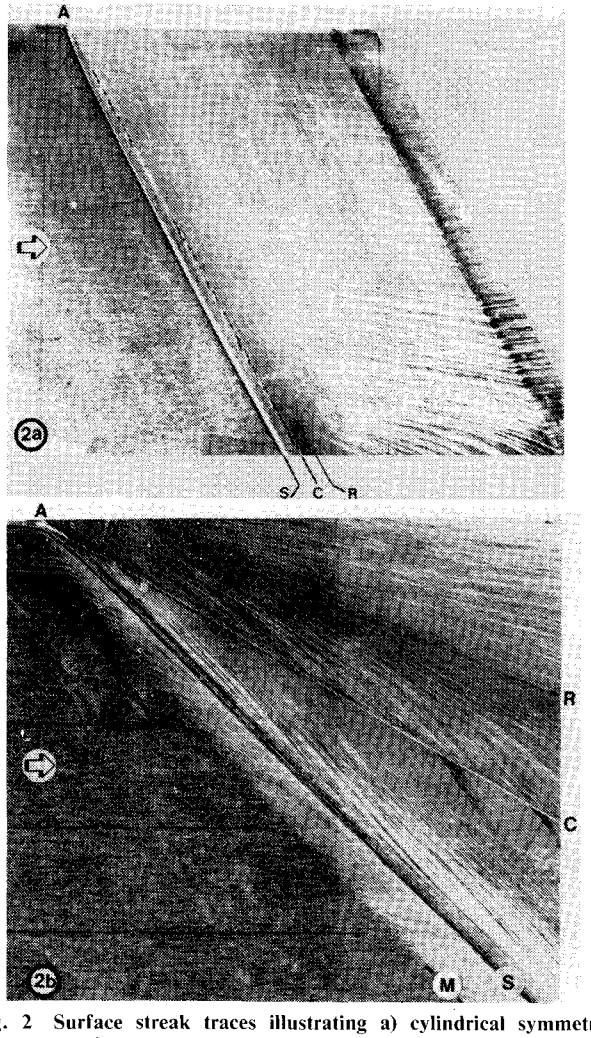

Fig. 2 Surface streak traces illustrating a) cylindrical symmetry ($\alpha_s=16$ deg, $\lambda=30$ deg), and b) conical symmetry ($\alpha_s=24$ deg, $\lambda=60$ deg).

Results and Discussion

Topography of Flow Regimes

As mentioned earlier, the impetus for the present study was the observation that systematically sweeping back an initially 2D compression corner leads first to an asymptotically cylindrical interaction symmetry followed eventually by an asymptotically conical symmetry. Here, cylindrical symmetry means that the upstream influence line runs parallel to the swept corner line, while conical symmetry means that the upstream influence line and the corner line belong to a family of lines having a common origin. Examples of kerosene-lampblack surface streak traces for both flow regimes are given in Fig. 2. The regimes are asymptotic in the sense that an inception length from the model apex is required before either cylindrical or conical conditions are established. Thus, strictly speaking, the overall flow patterns should be termed quasi-cylindrical and quasi-conical respectively.

It is helpful to analyze the topography of these flow regimes by constructing the schematic diagrams of surface streak lines shown in Fig. 3. Their salient features are lines of 3D separation and reattachment which presumably spring from a microscopic saddle/nodal point pair at the model apex.[11] The onset of the 3D interaction is marked by a line of maximum upstream influence designated "M" in Fig. 3, which is defined even in the few present results where no separation is evident. Finally, the inception zone near the model apex is characterized by a length along the corner line, L_i, required to establish cylindrical or conical symmetry, and by the upstream influence L_{mi} at the end of this zone.

For simplification the surface patterns of Fig. 3 have been divided into five zones: 1) incoming 2D flow, 2) inception zone, 3) zone of cylindrical or conical upstream influence, 4) downstream zone between corner and reattachment lines, and 5) outgoing flow. The present attention is mainly directed at zone 3.

Interaction Zone 3: Cylindrical and Conical Regimes

Referring to Fig. 3a, the shaded cylindrical upstream influence zone is completely characterized by the definition of cylindrical symmetry and by the lengths L_i and L_{mi}, which define where it begins and its size. In contrast, the conical upstream influence zone (shaded in Fig. 3b) has no characteristic size by definition. It can be specified, however, by a virtual origin and L_{mi}, or by the sweepback angle of the upstream influence line. Note that the inception zone is generally convex to the oncoming flow and of finite size, so the virtual conical origin lies above the model apex by some distance Δz.

Given these defining parameters, the data set of surface streak patterns is examined for cylindrical or conical symmetry by fitting a straight line to the asymptotic locus of the upstream influence. If this line is parallel to the swept corner line (within narrow limits necessitated by the nonuniformity of δ_i with z), then the upstream influence is asymptotically cylindrical. Divergence of these lines similarly denotes asymptotic conical flow. (A third possibility—convergence of the lines—was not observed in any of the experimental results.) This procedure also yields values of L_i, L_{mi}, and Δz for each test point.

The validity of this procedure is verified by comparing the measured surface pressure distributions at various transverse distances in Cartesian and spherical coordinates. Fig. 4a confirms the quasi-two-dimensionality of a sample cylindrical flow, using the corner location for the $x=0$ reference. In Fig. 4b, conical pressure distributions are correlated by normalizing the x axis by the distance from the virtual origin, $z+\Delta z$. These results significantly demonstrate that the concept of cylindrical and conical symmetry encompasses more than just the upstream influence zone.

A Criterion for the Cylindrical/Conical Boundary

Having now developed criteria to specify both cylindrical and conical interaction regimes, it remains to find an additional criterion for the boundary between the two. Initially, this process seems clouded by the observation that, as λ is increased systematically from 0 deg, the inception length L_i to cylindrical flow increases without bound. Similarly, as λ is decreased systematically from large values the inception length to conical flow increases without bound. Thus the process described earlier of distinguishing between cylindrical and conical regimes becomes more difficult the closer the boundary is approached.

The solution to this problem lies in the very nature of the inception length, L_i: that it can be used to form a criterion for the cylindrical/conical boundary because it has singular points (poles) on that boundary. This is demonstrated in Fig. 5, where L_i is plotted vs λ with α_s as a parameter. The inset of the figure shows schematically how the singular behavior of L_i near the boundary is used to define a critical sweepback angle, $\lambda_{cr}(\alpha_s)$, on the boundary. This boundary criterion may be written symbolically as

$$\lim_{L_i \to \infty} \lambda_{cy} = \lim_{L_i \to \infty} \lambda_{co} = \lambda_{cr}(\alpha_s) \tag{1}$$

Thus, a swept corner interaction with a given value of α_s and the corresponding critical sweepback angle, λ_{cr}, exhibits neither cylindrical nor conical symmetry. Instead, the 3D inception zone with its curved upstream influence line extends indefinitely in the spanwise direction. Since all practical wind tunnels have limited spanwise dimensions, it follows that

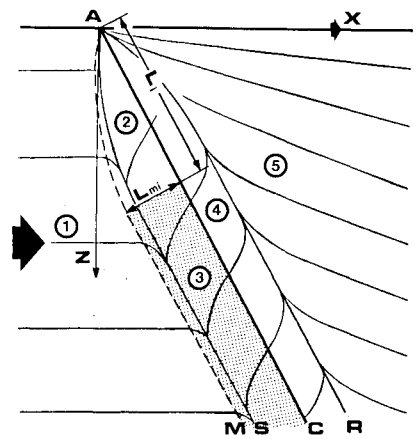

Fig. 3a Schematic of surface streak lines for asymptotically cylindrical interaction.

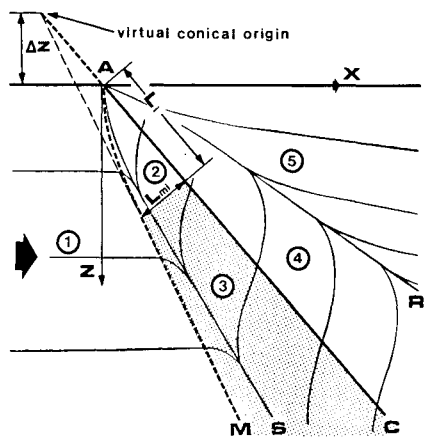

Fig. 3b Schematic of surface streak lines for asymptotically conical interaction.

$\lambda_{cr}(\alpha_s)$, which defines the cylindrical/conical boundary, can only be determined within a finite uncertainty band. For the present tests this band is ± 2.5 deg or $\pm 4\%$ of the range of λ covered in the test matrix.

Cylindrical/Conical Boundary

Using the criterion of Eq. (1), the data of Fig. 5 yield five values of λ_{cr} on the cylindrical/conical boundary, corresponding to the five values of α_s in the test matrix. This result effectively defines the boundary for swept corner interactions at $M_\infty = 2.95$, as illustrated in Fig. 6. Also shown are the 34 (α_s, λ) points tested, with each coded to indicate either cylindrical or conical symmetry. Figure 6 clearly shows that the regime boundary is a strong function of both λ and α_s. That is, for higher values of α_s the cylindrical/conical boundary occurs much earlier in the sweepback process.

A Hypothetical Mechanism for the Boundary

Up to this point the authors had postulated two rival mechanisms to explain the cylindrical/conical boundary. The first mechanism assumes a fundamental change in the mass balance of entrained and ventilated fluid in the 3D separation region,[12] while the second assumes an intimate connection with the inviscid shock detachment phenomenon. As shown in Fig. 7, the experimental results give rather strong support to the second hypothesis.

Figure 7 shows the observed $M_\infty = 2.95$ cylindrical/conical boundary with superimposed curves for inviscid shock detachment at $M_\infty = 3.0$, 2.4, and 2.0. These curves were computed by taking the flat plate of Fig. 1 as the plane of symmetry, ignoring the boundary layer for the moment, and thus modeling the swept corner flow as a symmetrical delta wing in a uniform incoming flow at M_∞. The 2D oblique shock relations resolved normal to the wing leading edge are known to apply in this case.[13]

The comparison in Fig. 7 shows a striking similarity between the observed cylindrical/conical boundary and the inviscid detachment curves. However, the Mach number for which the boundary and the detachment conditions agree most closely is not that of the actual experiments ($M_\infty = 2.95$), but rather a lower value of about 2.2. This is a natural consequence of the fact that, because of the turbulent boundary layer, the true incoming flow of the experiments has a nonuniform Mach number distribution.

Some progress has recently been made in modeling 2D shock/turbulent boundary-layer interactions by treating most of the incoming boundary layer as a nonuniform inviscid field.[14,15] (In fact, this is the basis of the well-known "triple-deck" theory.) These analytical schemes recognize that the decreasing Mach number toward the wall in the supersonic turbulent boundary layer, although a result of turbulent momentum transfer, can be modeled largely as an inviscid rotational flow. The significant effects of viscosity are thus

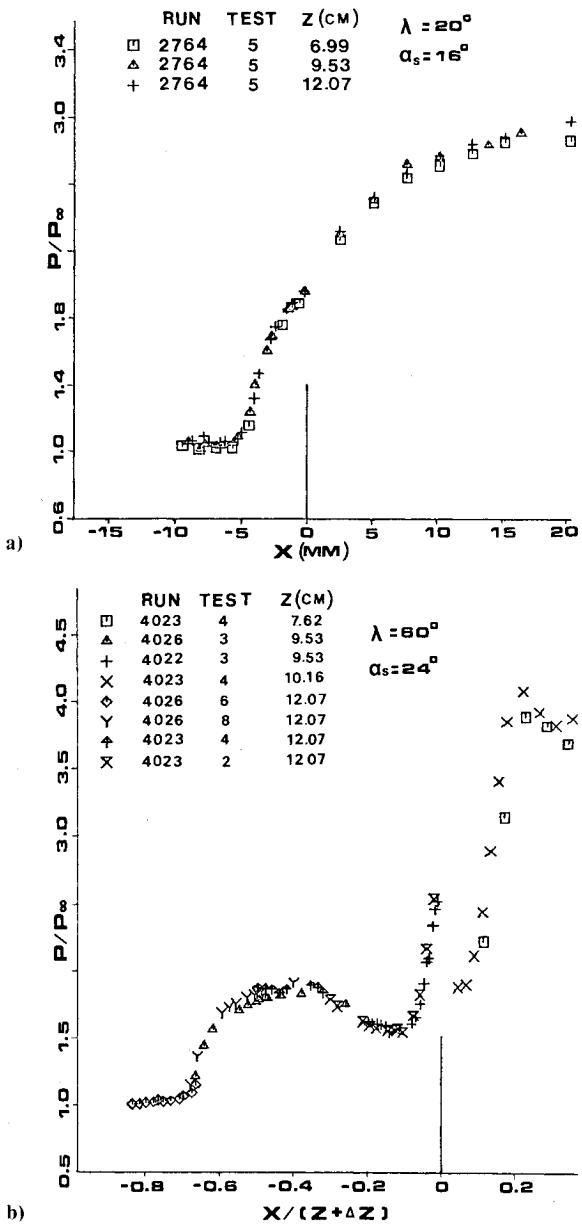

Fig. 4 Surface pressure distributions correlated for a) cylindrical flow, and b) conical flow.

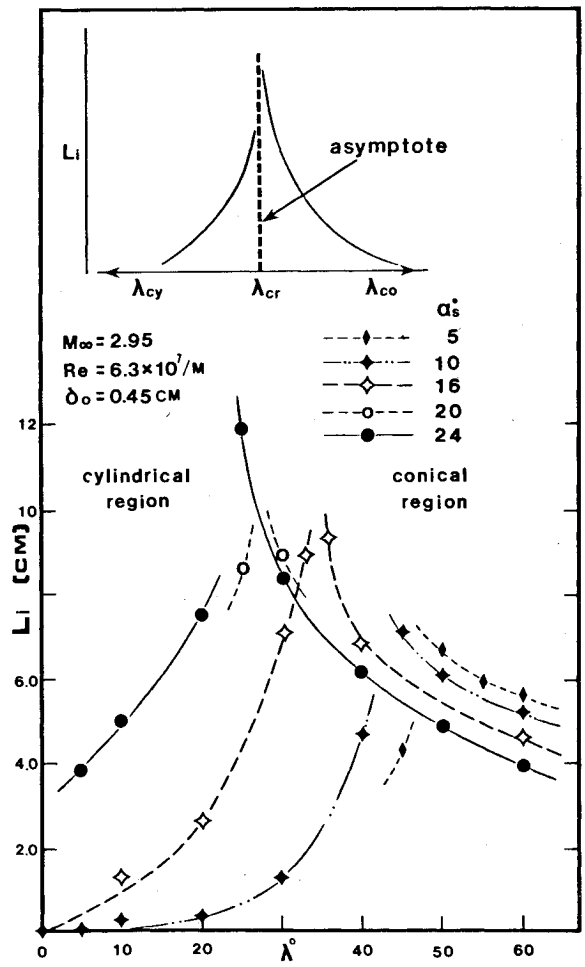

Fig. 5 Plot of inception length vs sweepback angle illustrating criterion for cylindrical/conical boundary.

confined to a thin region—the "inner deck"—at the bottom of the boundary layer.

For present purposes this philosophy dictates that M_∞ is not the Mach number at which shock detachment first occurs in a swept compression corner interaction. Rather, it is some effective Mach number near the wall (also called M_{slip}[14,15]) which marks the boundary between viscous and inviscid rotational domains, and is presumably responsible for the onset of shock detachment.

If one hypothesizes a cause-and-effect relationship between detachment and the cylindrical/conical flow regime boundary, then Fig. 7 indicates that the effective Mach number for detachment is in the range of Mach 2.1 to 2.3 for $M_\infty = 2.95$. It is difficult to verify this range on independent grounds, since the nature of M_{slip} is not well understood. However, Rosen et al.[14] have developed a 2D calculation method based on the above inviscid-flow reasoning, and their results indicate that $2.1 \leq M_{slip} \leq 2.3$ is not unreasonable for the present test conditions.

The role of M_{slip} in the shock detachment process is clearly an important one that cannot be fully specified at present. However, note that Rosen et al. show M_{slip} not to be a sole function of the incoming boundary layer, but to depend upon the compression corner angle as well. This might contribute to the observed fact that the cylindrical/conical boundary in Fig. 7 does not fall exactly along a single detachment curve. In any case, the detailed correspondence between M_{slip} and shock detachment at a swept compression corner is an important subject for ongoing study.

Returning to the hypothesized mechanism of the cylindrical/conical boundary based on inviscid shock detachment, we have now heuristically modified it to include the nonuniform field of the incoming turbulent boundary layer. The result appears most clearly when the information in Fig. 7 is presented in normalized form. Recognizing that the intersections of the detachment curves with the abscissa of Fig. 7 are 2D shock detachment angles at M_∞, while those with the ordinate are Mach angles at M_∞, an appropriate normalization has been performed in Fig. 8 to essentially remove the M_∞ dependence. The present cylindrical/conical boundary data are superimposed on the invsicid detachment curves through the assumption that $M_{slip} = 2.2$. An excellent correspondence between the two is evident everywhere except at the highest value of α_s/α_{dt}. Here, to be demonstrated later, the dimensional limits of the experimental corner models begin to play an active role.

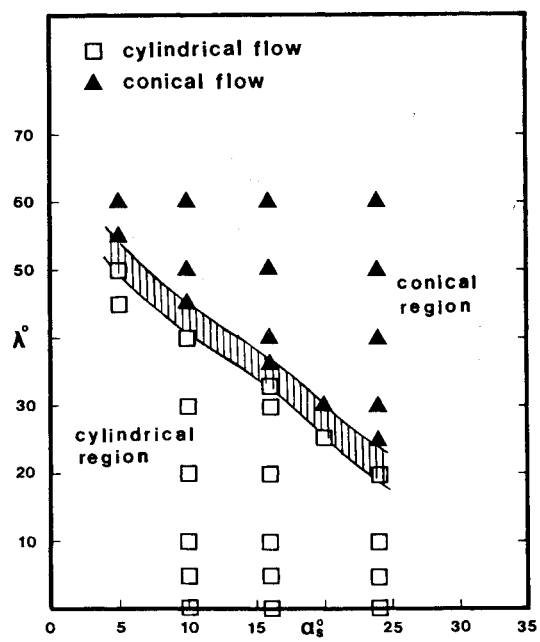

Fig. 6 The cylindrical/conical flow regime boundary for swept corner interactions at $M_\infty = 2.95$.

The Physical Basis of the Detachment Hypothesis

Inviscid shock detachment is proposed in the previous section as a hypothetical mechanism for the cylindrical/conical interaction boundary, and a similarity between the two conditions is demonstrated. A plausible physical explanation can be made as well. It is one that has been invoked many times in the past: that *the inviscid shock location is the proper reference from which to measure the extent of a shock/boundary layer interaction.* Almost every investigator of shock waves impinging on a planar boundary layer has made this assumption for lack of any other reference location, though investigators of compression corners and similar flows have chosen the corner line as a more convenient reference. In

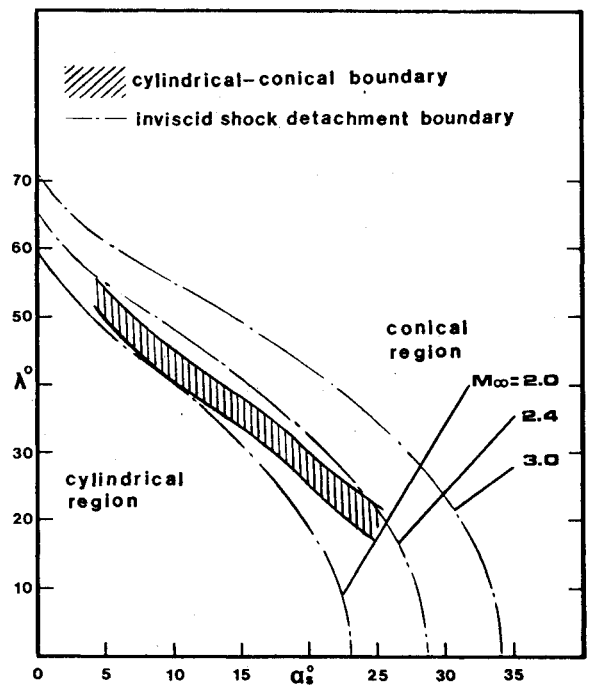

Fig. 7 Comparison of cylindrical/conical boundary and inviscid shock detachment curves.

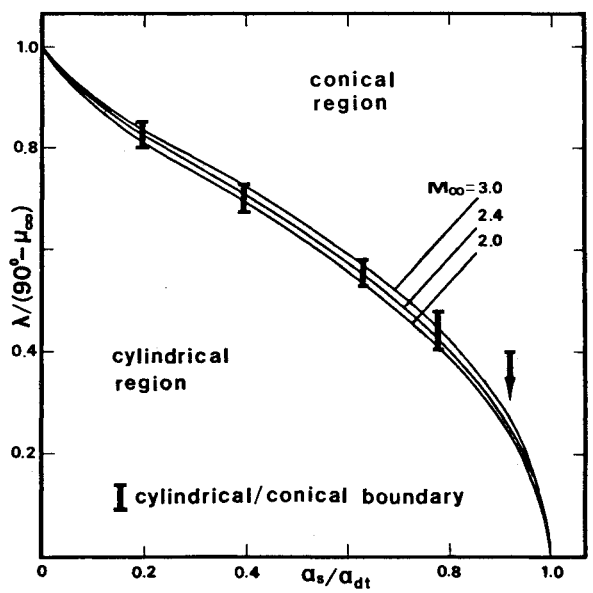

Fig. 8 Comparison of cylindrical/conical boundary with inviscid shock detachment in normalized coordinates.

fact the two choices are equivalent only when the inviscid shock remains attached to the corner.

When this is the case, even for swept corner flows, the inviscid constraints imposed upon the boundary layer by the outer flow are locally planar at the corner. Neither the shock strength nor its relationship to the corner varies in the spanwise direction. This encourages the development of a cylindrical shock/boundary layer interaction.

On the other hand, once the sweepback angle is increased to the point of shock detachment, swept corners of semi-infinite dimensions produce conical inviscid flows. While the shock generally remains attached at the apex, its trace in the plane of the boundary layer diverges conically from the corner line with increasing span. The upstream influence measured from the corner line must necessarily then be asymptotically conical. This provides a straightforward physical basis on which to connect shock detachment with the observed cylindrical/conical boundary. It also agrees with all the present experimental observations except those where finite dimensional limits come into play.

The Limits of Planar and Conical Flows

Thus far, dimensional limits of the test models have been largely excluded from consideration. There is good reason to expect, for models of less than semi-infinite extent, that the model dimensions will play an important part in the shock/boundary layer interaction scaling (see, for example, the study of blunt fin-induced interactions by Dolling and Bogdonoff[16]). There has been no intention to study such effects in the present work, and the test models were deliberately designed to be semi-infinite in order to avoid them.

However, dimensional effects eventually become unavoidable as one proceeds toward the lower right-hand quadrant of Fig. 8 along the shock detachment curves. In this case the total Mach number behind the inviscid shock rapidly approaches unity, whereupon the influence of both finite model span and height begin to play an important role in determining the shock shape.

Once this occurs, the detached shock generated by a test model will no longer be conical. Although conical bodies always support conical shocks when the flow is everywhere supersonic, the definition of such a flow naturally includes no linear dimension.[17] Thus, once the dimensional limits of a test model are sensed by the flow, the shock envelope will revert from conical to cylindrical symmetry wherein the shock standoff distance is determined by the significant model dimension. (See for example, Zheltovodov.[10])

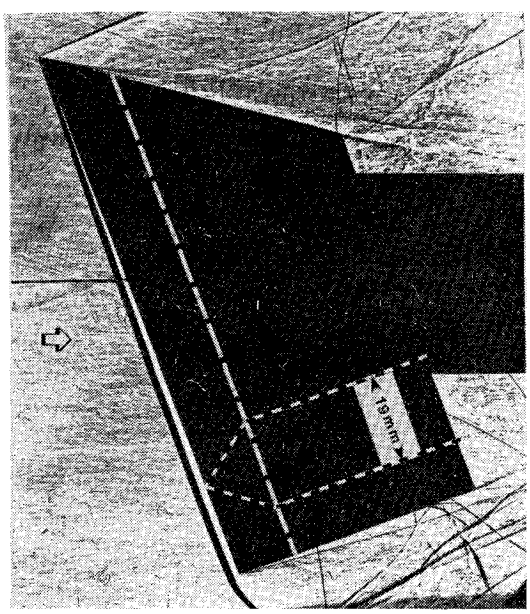

Fig. 9 Shadowgram showing detached shock shape of symmetrical wedge with $\alpha_N = 40$ deg and $\lambda = 20$ deg, $M_\infty = 2.95$. (Cross section shown by dotted lines.)

An example of this phenomenon is shown by the shadowgram of Fig. 9. The shock wave about this symmetrical swept wedge model is attached at the apex but detached elsewhere along the leading edge. Initially it diverges conically from the leading edge, but soon the effects of finite model dimensions are felt and the shock turns parallel to the leading edge.

Similar inviscid effects occur at the upper limit of α_s in the present experiments. Over the range of 5 deg $\leq \alpha_s \leq 20$ deg the authors have verified that the experiments are semi-infinite by making conservative estimates of the propagation of disturbances from the height and span limits of the test models. However, the lower limit of the cylindrical/conical boundary for $\alpha_s = 24$ deg in Figs. 6-8 is indeterminate due to possible dimensional influences. Further, a few tests at an even larger value of α_s (28 deg) showed obvious effects of the model dimensions, causing the apparent cylindrical/conical boundary to tend toward a constant value of λ_{cr} with increasing α_s. No practical semi-infinite experiment can proceed much further into this region, and it is here that the present consideration stops. The topic of dimensionally dominated 3D interaction scaling is a separate and important one for future study.

No such dimensional limitations are met at the low end of the α_s range, however, although no tests were made at $\alpha_s < 5$ deg due to increasing difficulties with model fabrication and data interpretation. Nonetheless, it seems entirely reasonable to extrapolate the cylindrical/conical boundary to $\lambda = 90$ deg $- \mu_\infty$ at $\alpha_s = 0$ deg in Figs. 6-8.

Effect of Incoming Flow Variations on the Boundary

There remains the question of whether or not changes of Re_δ or M_∞ in the incoming flow affect the observed cylindrical/conical boundary, thus limiting its generality. As far as Re_δ is concerned, the previous work of Settles et al.[6] indicates that there should be no such effect.

Settles formulated a general scaling law accounting for Re_δ effects. The result, which has now been verified for several different 3D interactions,[6,18,19] shows that Re_δ variations cause a uniform expansion or compression of the "footprint" of an interaction without changing its shape. Thus Re_δ variations in the incoming flow are not expected to affect the observed cylindrical/conical boundary.

To verify this, a limited series of swept corner experiments with 11 (α_s, λ) combinations was carried out on the floor of the 20×20 cm tunnel. Here δ_0 is five times as large as in the main body of experiments carried out on the flat plate. Further, a few checks of the Re effect were made with a higher Re value of 18.9×10^7/m. In both cases the cylindrical/conical boundary of Figs. 6-8 remained invariant to changes of incoming-flow Re_δ.

A potential difficulty was mentioned earlier concerning the nonuniform δ_ℓ at the beginning of a highly swept corner interaction. This effect arises because of the 2D turbulent boundary-layer growth in the streamwise direction, and results in an increase of δ_ℓ with increasing distance along the swept corner line from the model apex. The effect is noticeable only at high sweep angles, where it tends to give an otherwise cylindrical interaction a slight spanwise growth of upstream influence.

In order to evaluate the influence of this growth on the determination of the cylindrical/conical boundary, it has been estimated using the scaling law of Ref. 6. The scaling law indicates that $L_m \sim \delta_\ell^{3/4}$ for the present test conditions. Given the magnitude of the spanwise growth of δ_ℓ, one can estimate the resulting incremental angular growth $\Delta\epsilon = \tan^{-1}[\Delta L_m/(z/\cos\lambda)]$ of the upstream influence line. Fortunately, this effect is found not to be significant for any of the present

test conditions. For example, at $\alpha_s = 24$ deg and $\lambda = 40$ deg, $\Delta\epsilon$ amounts to only 1.5 deg, which is well within the uncertainty band of the cylindrical/conical boundary.

Finally, there is the question of the M_∞ effect on the boundary. Based on the shock detachment hypothesis, this should be accounted for by the normalization of coordinates in Fig. 8. However, the required values of M_{slip} for interactions at arbitrary M_∞ can only be determined empirically at present. Further, a complete test of the detachment hypothesis requires data at a Mach number other than the present $M_\infty = 2.95$. Such experiments were not feasible in the present study, and remain to be done in future work.

Conclusion

A parametric set of experiments with semi-infinite swept-back compression corners has been carried out to address the question of cylindrical and conical symmetry in 3D shock/turbulent boundary-layer interactions. These interactions involve equilibrium, adiabatic turbulent boundary layers with a freestream Mach number of 2.95. The experiments encompass 34 combinations of compression corner sweepback angle and streamwise turning angle. The resulting data set includes both surface flow visualization and surface pressure measurements.

An analysis of the flow regime topography reveals that both cylindrically and conically symmetric 3D interactions can occur at the swept compression corners. Attention is centered on these cylindrical and conical regimes, for which suitable defining criteria are developed. An additional criterion is then developed for the boundary between the two regimes, based on the singular behavior of the inception length to cylindrical or conical flow.

The resulting cylindrical/conical boundary appears to be directly related to the phenomenon of inviscid shock detachment from a swept corner. A hypothesis to that effect is formulated, incorporating an effective detachment Mach number smaller than M_∞ to account for the nonuniform profile of the turbulent boundary layer. Physically, this detachment hypothesis embodies the often-used assumption that the inviscid shock wave is the first-order determinant of interaction size and shape. It follows directly that cylindrical symmetry is associated with attached shocks and conical symmetry with detached shocks. The experimental results support this hypothesis up to extreme limits of compression corner turning angle, where no practical experiment can be performed without the influence of limited model dimensions.

Finally, the influence of changes in incoming flow Reynolds number and boundary-layer thickness is considered, and the observed cylindrical/conical boundary is found invariant to such changes. The effect of changes in M_∞ is less certain, however, requiring future work to fully test the detachment hypothesis, as well as to explore the nature of the effective Mach number for shock detachment.

Acknowledgments

This work was supported by the U.S. Air Force Office of Scientific Research under Contract F49620-81-K-0018, monitored by Dr. J. D. Wilson. The authors gratefully acknowledge useful discussions with Prof. S. M. Bogdonoff and also Prof. W. D. Hayes, who provided important insight into the nature of conical flows. We also note that Mr. G. Degrez of the von Kármán Institute was among the first to suggest that shock detachment might play a critical role in 3D interaction scaling.

References

[1] Green, J. E., "Interaction Between Shock Waves and Boundary Layers," *Progress in Aerospace Sciences*, Vol. 11, 1970, Pergamon Press, New York, pp. 235-340.

[2] Hankey, W. L. Jr. and Holden, M. S., "Two-Dimensional Shock-Wave Boundary Layer Interactions in High Speed Flows," AGARDograph 203, 1975.

[3] Stanewsky, E., "Shock-Boundary Layer Interaction in Transonic and Supersonic Flow," von Kármán Institute, Belgium, VKI-LS-59, 1973.

[4] Adamson, T. C. Jr. and Messiter, A. F., "Analysis of Two-Dimensional Interactions Between Shock Waves and Boundary Layers," *Annual Review of Fluid Mechanics*, Vol. 12, 1980, pp. 103-138.

[5] Settles, G. S, Perkins, J. J., and Bogdonoff, S. M., "Investigation of Three-Dimensional Shock/Boundary-Layer Interactions at Swept Compression Corners," *AIAA Journal*, Vol. 18, July 1980, pp. 779-785.

[6] Settles, G. S. and Bogdonoff, S. M., "Scaling of 2D and 3D Shock/Turbulent Boundary Layer Interactions at Compression Corners," *AIAA Journal*, Vol. 20, June 1982, pp. 782-789.

[7] Settles, G. S. and Teng, H.-Y., "Flow Visualization Methods for Separated Three-Dimensional Shock Wave Turbulent Boundary Layer Interactions," *AIAA Journal*, Vol. 21, March 1983, pp. 390-397.

[8] Stalker, R. J., "Sweepback Effects in Turbulent Boundary-Layer Shock-Wave Interaction," *Journal of the Aeronautical Sciences*, Vol. 27, May 1960, pp. 348-356.

[9] Zubin, M. A. and Ostapenko, N. A., "Structure of Flow in the Separation Region Resulting from Interaction of a Normal Shock Wave with a Boundary Layer in a Corner," *Izvestiya Akademii Nauk SSSR, Mekhanika Zhidkosti i Gaza*, No. 3, May-June 1979, pp. 51-58.

[10] Zheltovodov, A. A., "Properties of Two- and Three-Dimensional Separation Flows at Supersonic Velocities," *Izvestiya Akademii Nauk SSSR, Mekhanika Zhidkosti i Gaza*, No. 3, May-June 1979, pp. 42-50.

[11] Tobak, M. and Peake, D. J., "Topology of Three-Dimensional Separated Flows," NASA TM-81294, April 1981.

[12] Bradshaw, P., "Structure of Turbulence in Complex Flows," AGARD Lecture Series LS-94, 1978, Paper 10, p. 5.

[13] Narayan, K. Y., "The Flow Over a 'High' Aspect Ratio Gothic Wing at Supersonic Speeds," *Aeronautical Quarterly*, Vol. 26, Aug. 1975, pp. 189-201.

[14] Rosen, R., Roshko, A., and Pavish, D. L., "A Two-Layer Calculation for the Initial Interaction Region of an Unseparated Supersonic Turbulent Boundary Layer with a Ramp," AIAA Paper 80-0135, Jan. 1980.

[15] Melnik, R. E., "Turbulent Interactions on Airfoils at Transonic Speeds—Recent Developments," AGARD CP-291, Feb. 1981, Paper 10, p. 10-9.

[16] Dolling, D. S. and Bogdonoff, S. M., "Scaling of Interactions of Cylinders with Supersonic Turbulent Boundary Layers," *AIAA Journal*, Vol. 19, May 1981, pp. 655-657.

[17] Lighthill, M. J., "The Shock Strength in Supersonic 'Conical Fields,'" *Philosophical Magazine*, Vol. 40, 7th Series, 1949, pp. 1202-1223.

[18] Dolling, D. S. and Bogdonoff, S. M., "Upstream Influence Scaling of Sharp Fin-Induced Shock Wave Turbulent Boundary Layer Interactions," AIAA Paper 81-0336, Jan. 1981.

[19] Lu, F. K. and Settles, G. S., "Conical Similarity of Shock/Boundary Layer Interactions Generated by Swept Fins," AIAA Paper 83-1756, July 1983.